

Old Polyanionic Drug Suramin Suppresses Detrimental Cytotoxicity of the Host Defense Peptide LL-37

Mayra Quemé-Peña, Maria Ricci, Tünde Juhász, Kata Horváti, Szilvia Bősze, Beáta Biri-Kovács, Bálint Szeder, Ferenc Zsila, and Tamás Beke-Somfai*

Cite This: *ACS Pharmacol. Transl. Sci.* 2021, 4, 155–167

Read Online

ACCESS |

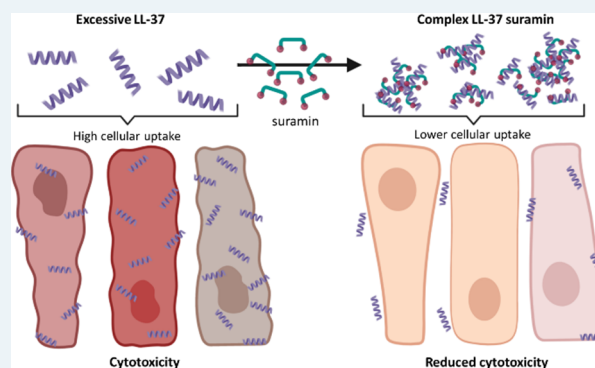
Metrics & More

Article Recommendations

Supporting Information

ABSTRACT: The host defense peptide LL-37 is the only human cathelicidin, characterized by pleiotropic activity ranging from immunological to anti-neoplastic functions. However, its over-expression has been associated with harmful inflammatory responses and apoptosis. Thus, for the latter cases, the development of strategies aiming to reduce LL-37 toxicity is highly desired as these have the potential to provide a viable solution. Here, we demonstrate that the reduction of LL-37 toxicity might be achieved by the impairment of its cell surface binding through interaction with small organic compounds that are able to alter the peptide conformation and minimize its cell penetration ability. In this regard, the performed cell viability and internalization studies showed a remarkable attenuation of LL-37 cytotoxicity toward colon and monocytic cells in the presence of the polysulfonated drug suramin. The mechanistic examinations of the molecular details indicated that this effect was coupled with the ability of suramin to alter LL-37 secondary structure *via* the formation of peptide–drug complexes. Moreover, a comparison with other therapeutic agents having common features unveiled the peculiar ability of suramin to optimize the binding to the peptide sequence. The newly discovered suramin action is hoped to inspire the elaboration of novel repurposing strategies aimed to reduce LL-37 cytotoxicity under pathological conditions.

KEYWORDS: cathelicidins, suramin, reduced cytotoxicity, molecular mechanisms, helical folding



INTRODUCTION

Among the host defense peptides (HDPs) produced by activated innate immune cells, cathelicidins play a pivotal role by having not only anti-microbial but also immunomodulatory action comprising both pro- and anti-inflammatory effects, the regulation of chemotaxis, and cell differentiation.^{1–3} In humans, cathelicidins are represented by LL-37 (Figure 1a), a 37-residue cationic peptide with not only anti-bacterial but also immunological and anti-neoplastic activity.^{4–8} It derives from the precursor hCAP18 (human 18-kDa cationic anti-microbial protein) as a result of the cleavage between an alanyl and a leucyl residue by proteinase 3.⁹

Human HDPs, which include histatins, defensins, and cathelicidins, are located at the surface of epithelial tissues for impeding the invasion of pathogenic microorganisms.^{10–12} In particular, LL-37 has been detected in various epithelia, including airway, skin, gastric, intestinal, and urogenital.^{5,13,14} It is also expressed in neutrophils,¹⁵ monocytes,¹⁶ T cells, B cells, and natural killer (NK) cells.¹⁷ Beside the membrane-damaging effect, the cathelicidins act through numerous complex mechanisms that include intracellular targets and the specific activation of several cell membrane receptors,⁴ suggesting an important role in host immunity homeostasis.

The anti-microbial and immunomodulatory actions rely on the structural and physicochemical properties of LL-37. Due to its cationic (net charge +6) and hydrophobic character, the peptide alters the lipid acyl chain packing, promoting the disruption of the anionic bacterial membrane.^{8,18–20} On the contrary, its hydrophobic nature enables the binding to membrane cell receptors, thereby mediating the immunomodulatory effects.^{21,22} Note that, although LL-37 preferentially perturbs bacterial membranes, it interacts also with eukaryotic cell membranes, and high peptide concentrations can thus cause cytotoxicity.^{8,23}

The concentration of hCAP18/LL-37, which is in the low micromolar range in healthy individuals,⁹ drastically increases in some pathological conditions, triggering cytotoxic effects.^{24–29} Indeed, LL-37 plays a role in the pathogenesis of several autoimmune diseases,³⁰ such as systemic lupus

Received: September 29, 2020

Published: December 3, 2020



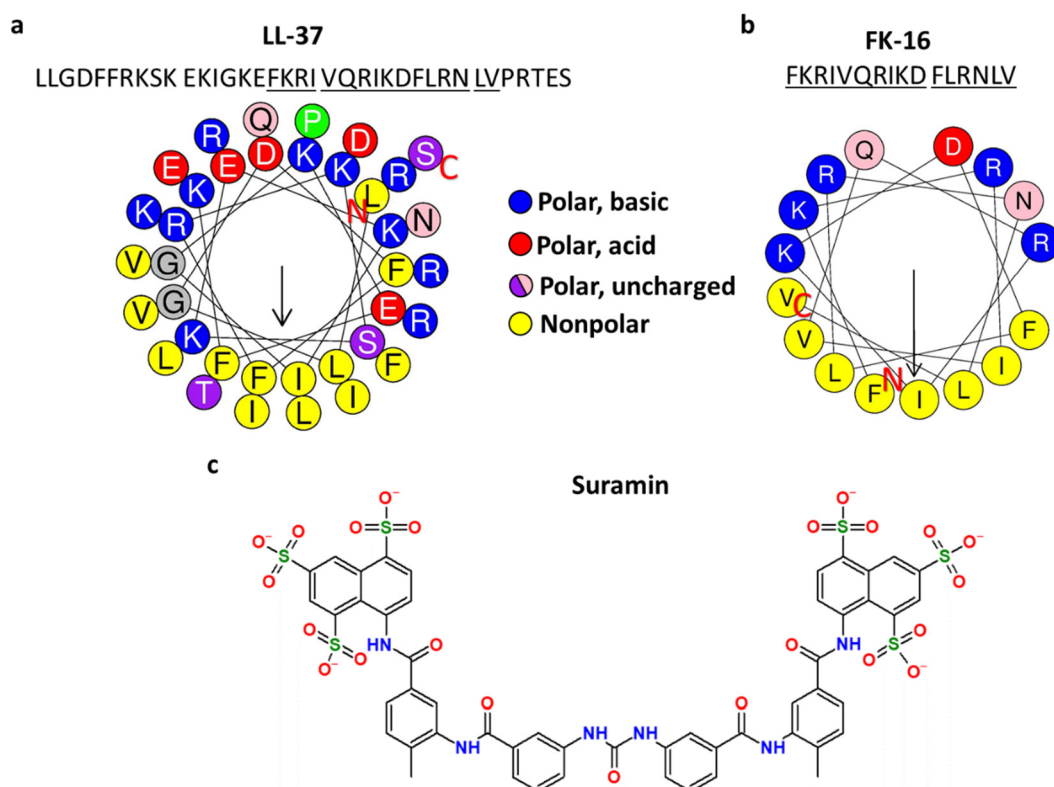


Figure 1. Chemical structures of the studied compounds. Helical wheel representations of peptides (a) LL-37 and (b) FK-16 drawn with HELIQUEST.⁷⁵ N and C indicate the N- and C-termini of the peptides. The underlined letters highlight the position of FK-16 sequence within that of LL-37. The arrows indicate the peptide hydrophobic face. The C-terminal of the peptide sequence is amidated. (c) Chemical structure of suramin.

erythematosus (SLE)³¹ and arthritis,³² where the over-expression of the cathelicidin leads to the activation of inflammatory pathways and apoptosis. Dysfunctional over-expression of LL-37 can amplify a local inflammatory response in common skin diseases, including psoriasis^{33,34} and rosacea.^{35,36} Further on, the cathelicidin expression by intestinal epithelial cells is assumed to exert a protective effect against bacterial invasion.³⁷ However, an elevated level of LL-37 has been detected in the inflamed and noninflamed intestinal mucosa of patients affected by ulcerative colitis^{38,39} and Crohn's disease,³⁷ conditions known as inflammatory bowel disease (IBD). The biological complex role of LL-37 in IBD can be related to the regulation of inflammatory responses by affecting cytokine response and chemoattraction of inflammatory cells.^{10,38,40} In this regard, it should be noted that cathelicidins can influence the activity of immune cells, exacerbating inflammatory reactions.^{41,29} Since the over-expression of LL-37 can lead to undesirable cell dysfunction and disease pathogenesis, it would be highly important to find solutions that allow for its activity to be tightly regulated and thus reduce the harmful effect of dysregulated expression. It has been observed that an LL-37 interaction with some endogenous proteins affects peptide conformation, limiting its toxicity.^{42–44} Recent studies indicated that a rearrangement of the peptide structure might be required to bind to cell surface receptors.^{44,45} Related, our group has shown that similar conformational changes could be induced by interaction and noncovalent complex formation with different molecules, including anti-inflammatory drugs, porphyrin pigments, bile salts, and food dyes.⁴⁶ However, whether there is any potential

biological effect of such complex formations and how this may affect properties such as toxicity or cell internalization for LL-37 are not yet understood.

To address the latter key aspects, here, we selected the drug molecule suramin, which displayed the highest folding inducer effect on LL-37 out of the above set of molecules at a low ligand concentration, and investigated whether biological effects can be resulted for LL-37 from their interactions. Suramin (Figure 1c) is a polysulfonated naphthylurea compound with six negative charges that is known to interact with a variety of proteins, enzymes,⁴⁷ and also peptides.^{46,48}

Suramin was first introduced by Bayer in 1920, from a research program on ureas of the aminonaphthalene-sulfonic types and the anti-trypanosomal activity of azo dyes.^{49,50} It was tested during the following years to fight *Trypanosoma brucei rhodesiense* infections (also known as sleeping sickness)⁴⁹ and is still being used for treating the first stage of the acute disease.⁴⁷ Suramin has been repurposed for a large number of applications,⁴⁷ particularly regarding the treatment of several viral infections^{51–53} and the inhibition of the metastatic growth and angiogenesis of various neoplastic diseases including lung and pancreatic cancer.^{54–57} Moreover, due to its anti-purinerbic action, it is also considered as a promising candidate agent against the symptoms of autism spectrum disorder.^{58–60}

In this work, we investigated the potential of suramin in lowering LL-37 cytotoxicity, which would be beneficial in pathological conditions characterized by upregulated peptide expression. Moreover, a thorough analysis of the peptide structure was also performed in order to unravel the molecular mechanism underlying the alteration of its activity. In this

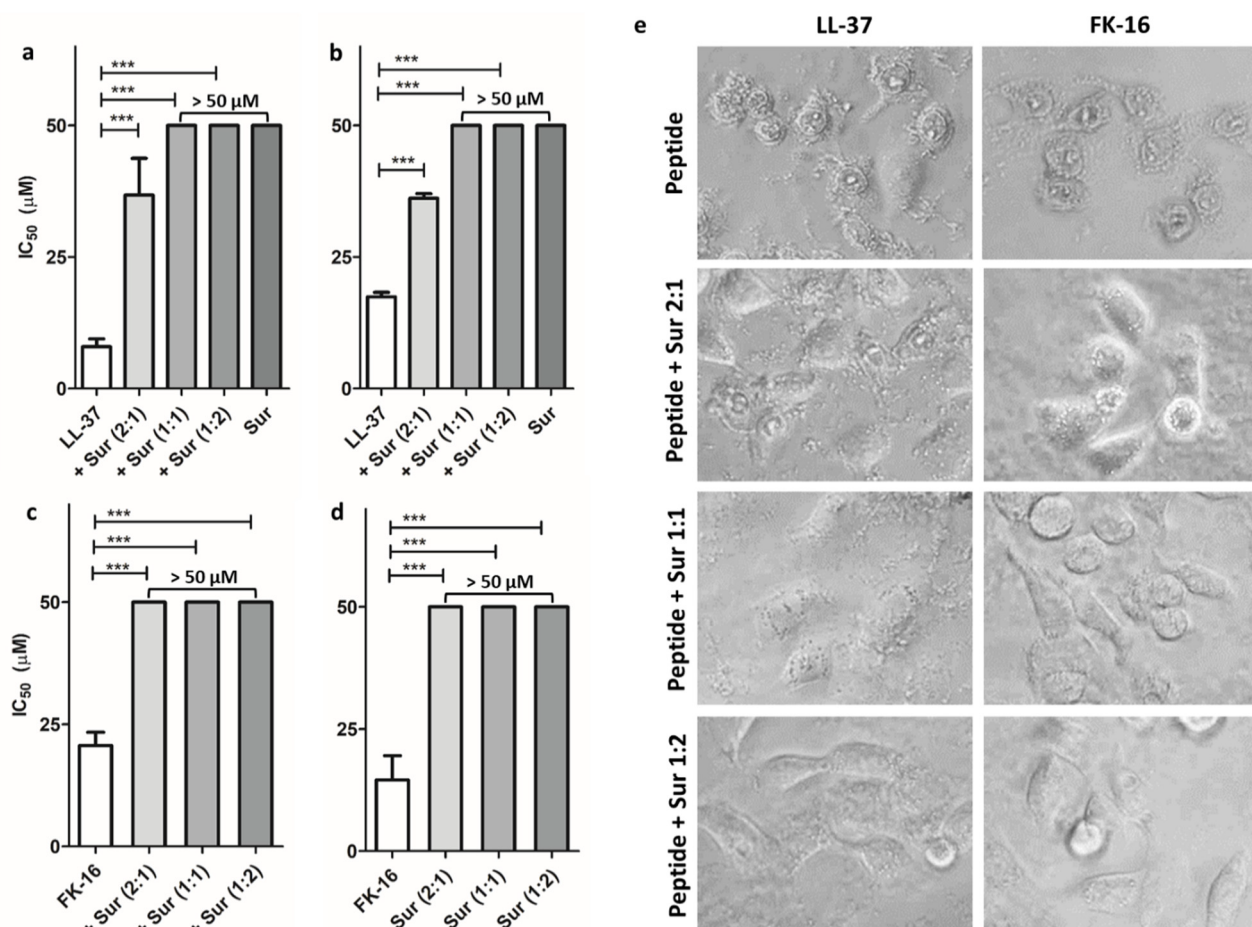


Figure 2. Effect of suramin on LL-37 and FK-16 cytotoxicity. (a and c) Cytotoxicity (4 h of treatment) and (b and d) cytotaxis (24 h of treatment) of LL-37 and FK-16 in the presence and absence of suramin (Sur) measured on HT-29 cells and presented by the mean IC_{50} values measured in three parallel experiments (***: $p < 0.001$). The results are presented as mean \pm SEM. The data indicated as “ $>50 \mu M$ ” are characterized by IC_{50} values higher than $50 \mu M$. The samples labeled as “+Sur $x:x$ ” correspond to the combination peptide + suramin at the specified peptide to drug molar ratio. (e) Microscopic images of HT-29 cells treated with $17 \mu M$ LL-37 or $33 \mu M$ FK-16 in the presence and absence of suramin at different peptide to drug molar ratios (2:1, 1:1, and 1:2). Cells were incubated with the studied peptides for 1.5 h at $37^\circ C$.

respect, an LL-37 fragment peptide, FK-16 (Figure 1b), which retains its anti-bacterial and anti-tumor activity,^{61,62} was also tested. Furthermore, in order to get mechanistic insights into the ability of suramin to affect the peptide structure and cytotoxicity, other small molecules bearing a net negative charge were studied, namely, brilliant blue G-250 (BBG), sulbenicillin (SBPC), and cefotetan (CTT). As with suramin, BBG is a sulfonated purinergic P2 receptor antagonist^{63,64} and, beyond its well-known use as a dye for staining proteins, it is also considered as a potential pharmacological agent for treating neuronal diseases.^{65–68} The monosulfonated SBPC is a broad-spectrum semisynthetic β -lactam antibiotic active against Gram-negative and Gram-positive bacteria^{69,70} that is extensively employed in many fields. CTT is a second generation cephalosporin that is particularly active against *Enterobacteriaceae*,^{71,72} which are the most frequent pathogens in gastrointestinal infections as well as ulcerative colitis and Crohn’s disease.^{73,74}

Results showed that the polysulfonated drug suramin significantly reduced the toxicity of LL-37 and its fragment FK-16 against monocytic and human colon cell lines while promoting the formation of complex associates and alteration of the peptide structure. This new action of suramin could

potentially be exploited in future drug repurposing projects in order to counteract cytotoxic effects due to the overexpression of LL-37. Furthermore, these results are also hoped to inspire exploration of the same drug–peptide interaction concept for other host defense peptides.

RESULTS AND DISCUSSION

Effect of Suramin on LL-37 and Its Fragment Cytotoxicity. The cytotoxicity of LL-37 was studied in the presence of suramin in order to unveil the potential effect of the drug on the cathelicidin toxic activity. In particular, the human colon HT-29 and the human monocytic MonoMac6 cell lines have been selected for this study as models for intestinal epithelial⁷⁶ and inflammatory cells,⁴¹ which are known to be involved in the cathelicidin expression and influenced by its action.^{5,13,41} The results from cell viability assays showed that the cytotoxicity of LL-37 on HT-29 cells is significantly prevented by the addition of suramin. After 4 h of treatment, a significant increase in the IC_{50} value at a 2:1 peptide to drug molar ratio (from 7.9 ± 3.0 to $36.8 \pm 14.0 \mu M$) and the complete prevention of peptide effect at higher suramin concentrations ($IC_{50} > 50 \mu M$) (Figure 2a) were measured. Similar results were observed after 24 h of treatment

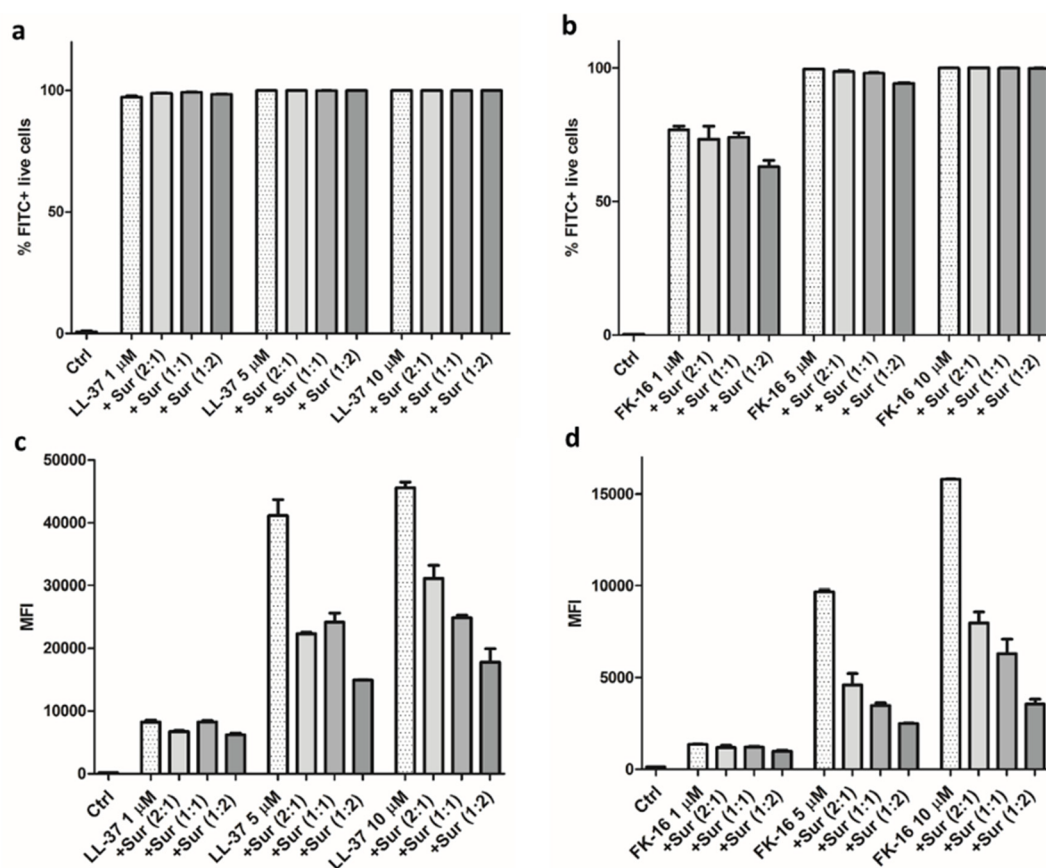


Figure 3. Peptide internalization. Cellular uptake of HT-29 cells assessed by flow cytometry using Cf-labeled LL-37 and FK-16 at 1, 5, and 10 μM concentrations in the presence and absence of suramin (Sur) at 2:1, 1:1, and 2:1 peptide to drug molar ratios. Percentage of cells containing Cf-peptide (Cf-positive cells, detected on FITC channel) and mean fluorescence intensity (MFI) values obtained for (a and c) Cf-LL-37 and (b and d) Cf-FK-16. The results are presented as mean \pm SEM.

when measuring the cytostatic effect, represented by a noticeable increase of HT-29 viability at the studied suramin concentrations (Figure 2b). The effect on the monocytic cells was even more significant (Figure S1), where IC_{50} values higher than 50 μM were detected starting from a 2:1 peptide to drug ratio for both 4 (Figure S1a) and 24 h treatments (Figure S1b). Interestingly, a similar effect of suramin was observed on the toxicity of the fragment FK-16 toward colon and monocytic cells, which was notably prevented starting from a 2:1 peptide to drug molar ratio ($\text{IC}_{50} > 50 \mu\text{M}$), regardless of the treatment duration (Figure 2c,d and Figure S1c,d).

The effect of suramin in attenuating the peptide cytotoxicity was also revealed by changes in the cell morphology (Figure 2e), as detected by bright field microscopic images. After 1.5 h of exposure, the HT-29 cells exhibited morphological alterations, resulting in a rough surface, shrinkage, and membrane protrusions, which are suggestive of possible apoptotic processes. Noticeable differences could be visualized when the cells were treated with LL-37 in combination with suramin at a 2:1 peptide to drug ratio, namely, the disappearance of the surface alterations. The further increase of suramin concentration led to a marked prevention of cell damage on HT-29 cells, which showed a maintained membrane integrity with a smooth surface. Analogously, suramin inhibited almost entirely the cell damage caused by FK-16 already at a 2:1 peptide to drug ratio.

The morphological investigation demonstrated, in line with the cell viability test results (Figure 2a–d), the ability of suramin to prevent the impairment of HT-29 cell morphology and viability caused by both LL-37 and, in a similar manner, also by the fragment FK-16.

Peptide Cellular Uptake in the Presence of Suramin.

The cellular uptake of the carboxyfluorescein-labeled peptides was analyzed by flow cytometry on HT-29 cells. For performing these measurements, LL-37 and FK-16 were labeled with 5(6)-carboxyfluorescein (Cf) and measured at 1, 5, and 10 μM concentrations in the presence of suramin (2:1, 1:1, and 1:2 peptide to drug molar ratio) after 1.5 h of incubation. The percentage of FITC positive cells (containing Cf-peptide, detected on FITC channel) was near 100% for Cf-LL-37 at the studied concentrations, indicating a high-penetration ability (Figure 3a). As for the precursor peptide, a high internalization rate was detected also in the case of Cf-FK-16 (Figure 3b). However, the percentage of FITC positive cells was somewhat lower ($\sim 75\%$) at an 1 μM peptide concentration and reached $\sim 100\%$ at higher concentrations. The mean fluorescence intensity (MFI) factor was also considered for a comprehensive interpretation of the flow cytometry analysis, which showed increasing values at an elevated concentration of the Cf-peptides, indicating a dose dependent cellular uptake rate (Figure 3c,d). Interestingly, suramin caused a gradual decrease in the MFI values for both Cf-peptides, particularly visible at an 1:2 peptide to drug ratio

and probably suggesting the ability of the drug to prevent peptide internalization.

The analysis of flow cytometry data revealed a remarkable cellular uptake of Cf-LL-37 and Cf-FK-16 in HT-29 cells, both alone and in combination with suramin. Further analysis of the MFI values demonstrated that suramin hindered the internalization of Cf-LL-37 and Cf-FK-16, and this might be related with the reduction of peptide cytotoxicity observed in the presence of the polysulfonated drug.

In order to gain more insight into the internalization and localization of LL-37, HT-29 cells were monitored by confocal laser scanning microscopy after 1.5 h of incubation with the Cf-labeled peptide alone and in combination with suramin (Figure 4). In addition, nuclei and lysosomes were also stained. The results showed that Cf-LL-37 was localized in the cell membrane, cytosol, and vesicular compartments (probably endosomes) and was excluded from nuclei and lysosomes. In the presence of suramin at 2:1 and 1:2 peptide to drug ratios, Cf-LL-37 was visible at a lower extent compared to with the peptide alone. In accordance with flow cytometry results, confocal microscopy investigation suggested that suramin might be able to attenuate cellular internalization of the peptide, which could be sequestered from the cells with consequent prevention of its cytotoxicity.

Impact of Suramin on the Peptide Secondary Structure.

To understand the reasons underlying the above observations at the molecular level, the structural and the potential assembly formation aspects of the peptide–suramin interactions were investigated by circular dichroism (CD), infrared spectroscopy (IR), and dynamic light scattering (DLS). The far-UV CD curves of LL-37 in Tris buffer showed a prominent single negative band centered around 200 nm and a less intense shoulder located in the region 220–235 nm (Figure 5a, left panel). In accordance with the previous data, these spectral features indicated the peculiar unstructured conformation⁷⁷ of LL-37 in salt-free buffer.⁷⁸ It is, indeed, well-known that the cathelicidin structure is susceptible to inorganic anions,⁷⁸ adopting an α -helical conformation in response to the presence of ions such as phosphate, chloride, sulfate, and bicarbonate. The sequence of basic and acidic residues promotes the formation of salt bridges and renders the peptide prone to self-oligomerization.⁷⁹ Hence, the CD curve of LL-37 in physiological buffered salt solution (Figure 5b, left panel) already exhibited spectral patterns commonly observed for α -helical structures, namely, a positive–negative couplet (at \sim 198 and 208 nm) and a negative band at \sim 224 nm arising from π – π^* and n – π^* transitions, respectively. As reported in recent studies, suramin interacts with polycationic peptides, inducing folding of the natively disordered structure.^{46,48,80}

The effect of the polysulfonated drug on the peptide secondary structure was monitored upon the stepwise addition of suramin (Figure 5a, left panel). The titration resulted in spectral changes characterized by the progressive decrease of the amplitude and a red shift of the negative peak at \sim 200 to \sim 211 nm, together with the development of a positive band at \sim 198 nm and the increase of the intensity of the shoulder at \sim 227 nm. These changes occurred immediately after the suramin addition, suggesting a rapid interaction that resulted in a progressive increase of the peptide α -helix content. It is noteworthy that the spectral transformations are accompanied by a decrease of the intensity and deviation from the isosbestic point (\sim 209–211 nm), likely suggesting an association of the peptide chains. The intensity ratio CD_{222}/CD_{208} gradually

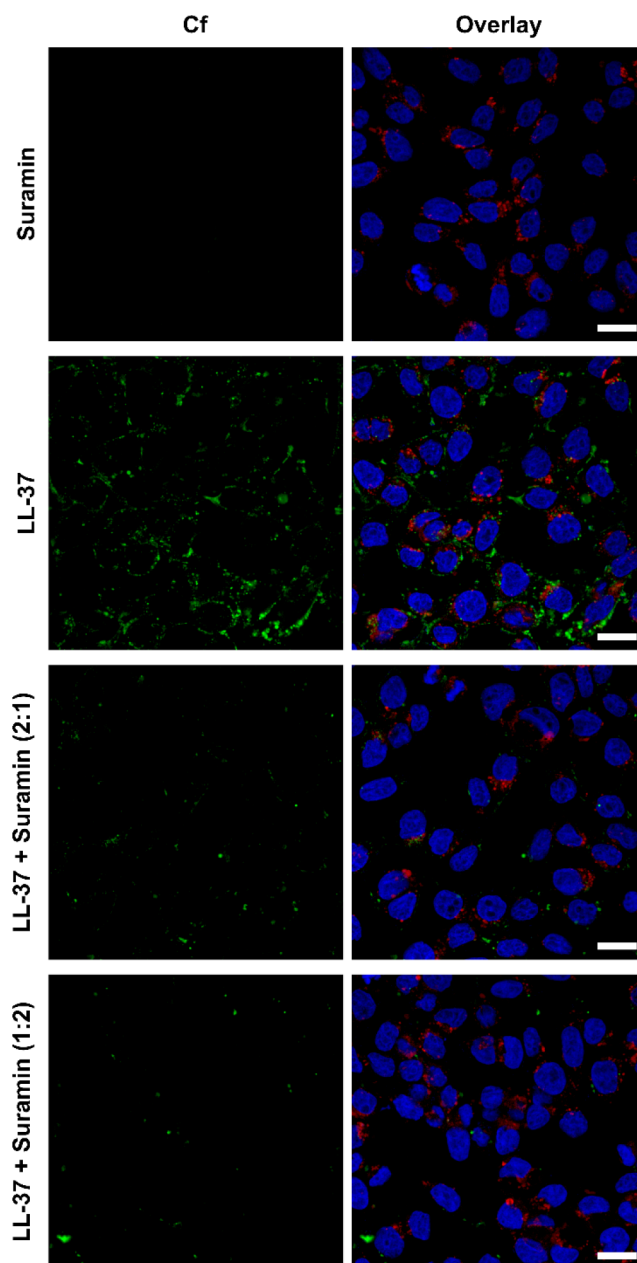


Figure 4. Cellular localization of LL-37. Confocal laser scanning microscopy visualizations of HT-29 cells incubated with LL-37 (1 μ M) in the absence and in combination with suramin at 2:1 and 1:2 peptide to drug molar ratios. Nuclei were stained with Hoechst 33334 (blue), the peptide was Cf-labeled (green), and lysosomes were stained with LysoTracker Deep Red (red). Scale bar: 20 μ M.

increased throughout the titration, denoting oligomerization of the peptide chains triggered by the progressive addition of suramin. In line with the CD results, the IR analysis of LL-37 amide I and II regions indicated an altered secondary and tertiary structure upon interaction with suramin (Figure 5a,b, right panels). Indeed, while modifications in the amide I bands are related with conformational changes,^{81–83} the slight variation of the intensity ratio amide I (\sim 1655 cm^{-1})/amide II (\sim 1545 cm^{-1}) is suggestive of an altered tertiary structure.⁸⁴ Under low-salt conditions (Figure 5a, right panel), the addition of 20 μ M suramin increased the prominent α -helix component (1654 cm^{-1}) at the expense of the shoulder (\sim 1680 cm^{-1}) representing intermolecular β -sheets and aggregated strands.

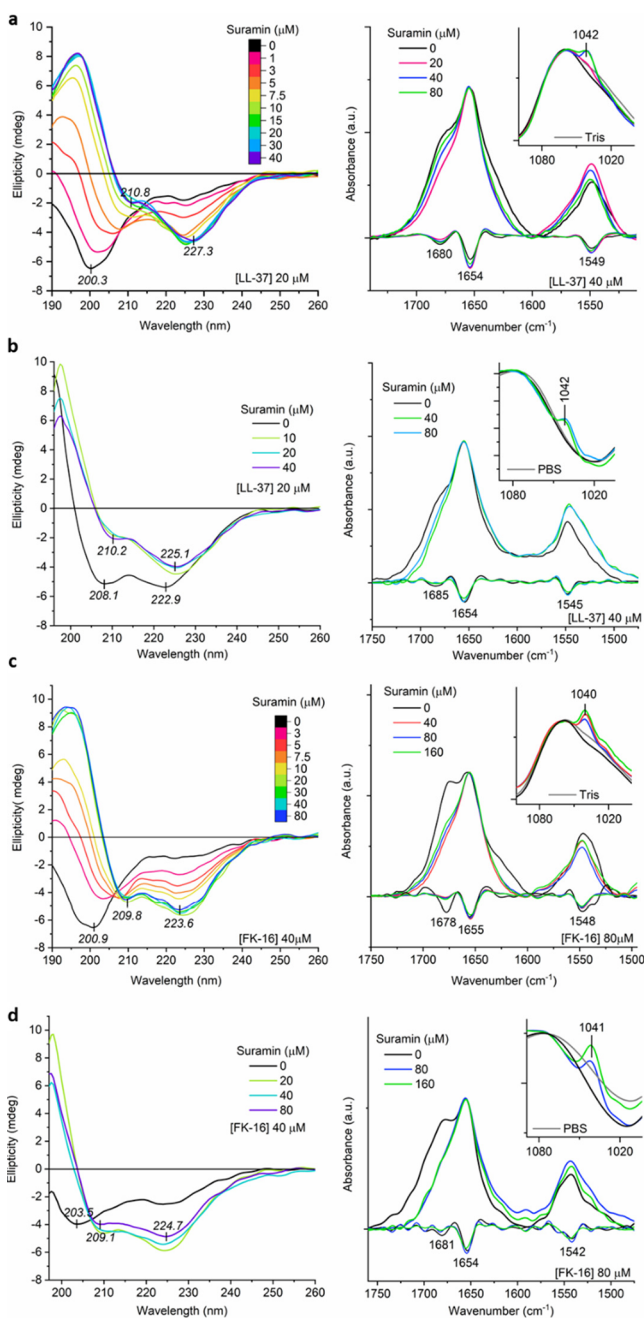


Figure 5. Structural changes of LL-37 and FK-16 driven by interaction with suramin. Left panels in a–d: far-UV CD spectra of peptides in the presence and absence of suramin in (a and c) Tris HCl buffer (10 mM, pH 7.4) or (b and d) PBS. Right panels in a–d: representative ATR-IR spectra in the amide region of peptides in the presence and absence of suramin in (a and c) Tris buffer or (b and d) PBS. Insets in a–d: in-phase S–O stretching of the sulfonyl groups ($\sim 1041\text{ cm}^{-1}$) characteristic of the complex formation peptide–suramin. Peptide spectra are normalized by the intensity at 1654 cm^{-1} in the amide region and at 1060 or 1080 cm^{-1} in the insets. Second derivatives are shown below and were used for peak identification.

Further, the suramin addition gradually enhanced the shoulder intensity, suggesting the occurrence of aggregation without reaching, however, the value detected for the peptide alone. Concurrently, it is possible to note the presence of a signal at 1042 cm^{-1} independent from the buffer vibrations (Figure 5a, inset right panel), which represent the in-phase S–O stretching

of suramin sulfonyl groups and can be considered as a marker for complex formation with the peptide.⁴⁸ As stated above, the presence of anions in PBS buffer induces α -helical folding of LL-37 (Figure 5b). Even if the peptide conformation did not significantly change in this case upon suramin addition, the intensity reduction of the CD curves accompanied by the increase of the CD_{222}/CD_{208} ratio is also suggestive of aggregation events triggered by the drug (Figure 5b, left panel). IR data indicated the peptide–drug complex formation (1042 cm^{-1}) also in PBS buffer (Figure 5b, inset right panel). Moreover, in agreement with CD results, the analysis of the amide I band suggested that the α -helical conformation in PBS buffer remained predominant at increasing suramin concentrations (Figure 5b, inset right panel).

A similar increase of α -helicity upon the stepwise addition of suramin can be observed for the 16-residue fragment FK-16 in Tris buffer (Figure 5c, left panel). The CD_{222}/CD_{208} intensity ratio suggests, similarly to the case of LL-37, the association of the peptide chains, although on a smaller scale compared to the 37-residue precursor peptide. IR spectroscopy is consistent with the CD results, showing the narrowing of the amide I vibration in the presence of suramin, which is indicative of increased peptide helicity (Figure 5c, right panel). Contrary to the full-length peptide, FK-16 is unstructured in PBS buffer and experiences a transition to a predominantly helical conformation upon the addition of suramin (Figure 5d, left panel). The presence of the infrared spectroscopic marker at $\sim 1041\text{ cm}^{-1}$ indicated the formation of the complex FK-16–suramin at the studied concentrations, both in Tris and PBS buffers (Figure 5c,d, insets right panels).

The formation of peptide–suramin molecular associates, in Tris as well as in PBS, was also supported by light scattering methods (Figure S2). In the presence of suramin, it was possible to observe an increase of the amplitude together with a shift of the correlation function to higher decay times, which implies a transition to larger hydrodynamic diameters in the micrometer range. It can be noted that the LL-37 interaction with suramin in PBS led to larger assemblies compared to those in the case of FK-16. This might be related to the larger size of the precursor peptide, nonetheless to the peculiar self-association propensity of LL-37 under physiological conditions.⁷⁹ The formation of large associates is in line with previous observations of peptide–suramin interaction, in which the molecular complexes showed a definite characteristic morphology.⁴⁸

The electrostatic interactions between the positively charged residues of LL-37 (+6) and the negatively charged groups of suramin (–6) presumably play an important role in the folding of the peptide and initiate the formation of the complex.^{46,48} It has been suggested⁴⁶ that suramin insertion among the cationic side chains might decrease the repulsive ionic forces between them, enabling helix formation and peptide folding. This might also apply to the shorter derivative FK-16, which bears five positive charges and experiences similar helical folding.

Mechanistic Considerations of Suramin Compared to Other Drug Molecules. Recent studies in our group have demonstrated that some bioactive small compounds are able to alter the secondary structure of cationic peptides, resulting in either the enhancement or inhibition of their biological activity. For instance, the azo-dye tartrazine demonstrated to form complexes with the histatin-derived peptide DHVAR4, resulting in improved perturbation of the bacterial membrane

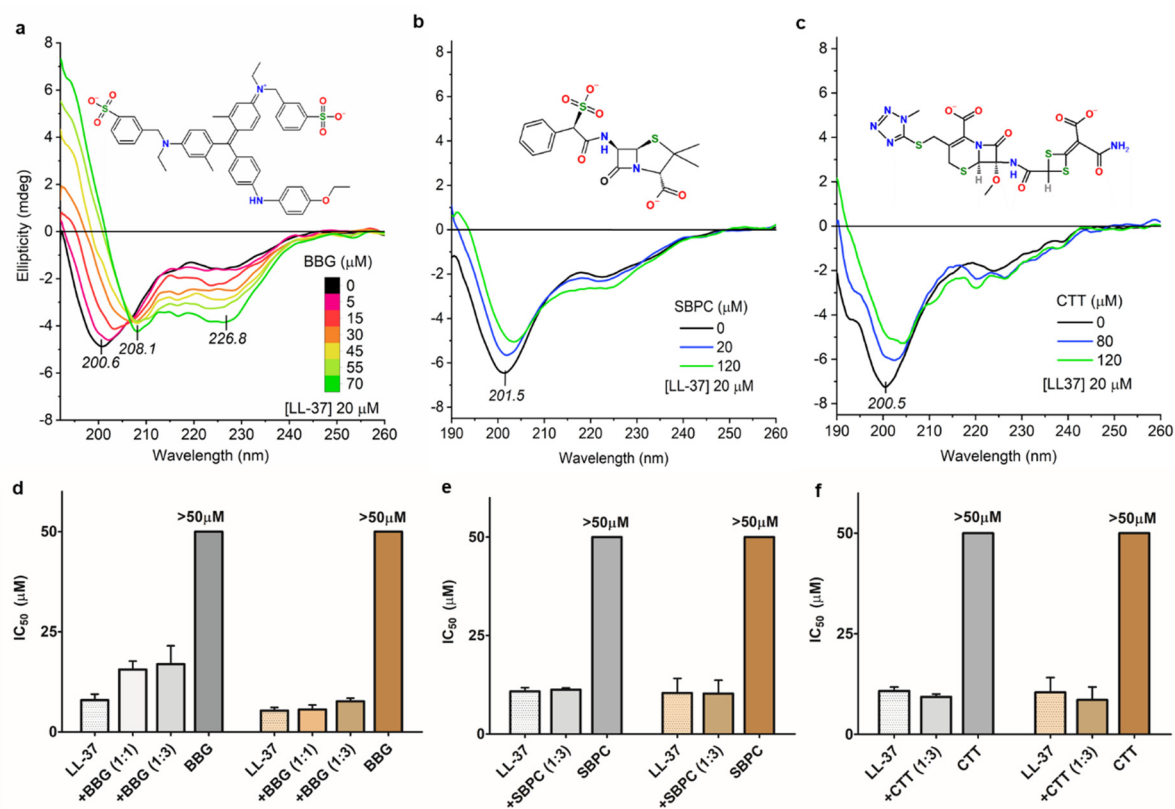


Figure 6. Influence of BBG, SBPC, and CTT on LL-37 conformation and cytotoxicity. (a) Far-UV CD spectra of LL-37 in Tris HCl buffer (pH 7.4) upon stepwise addition of BBG. (b and c) Far-UV CD spectra of LL-37 in Tris HCl buffer (pH 7.4) and in the presence of 20 or 80 and 120 μM SBPC or CTT. (d) Cytotoxicity (gray bars) and cytostasis (orange bars), presented by the IC₅₀ values of LL-37 alone and in the presence of BBG at 1:1 and 1:3 peptide/BBG ratios measured on HT-29 cells. (e and f) Cytotoxicity (gray bars) and cytostasis (orange bars) of LL-37 alone and in the presence of SBPC or CTT at an 1:3 peptide to drug ratio measured on MonoMac6 cells.

integrity and consequent enhancement of its anti-bacterial action.⁸⁵ Somewhat different is the case of suramin, which has shown to induce folding and form complexes with the cecropin/melittin hybrid peptide CM15, preventing its anti-microbial and cytotoxic activity.⁴⁸ In this study, we report a similar action of suramin on LL-37. The interaction led to the formation of complexes with low-cell-internalization ability; hence, the peptide was sequestered from the cells and its toxic action was prevented accordingly.

In order to understand the mechanistic aspects, the structural and biological impact of suramin on LL-37 has been compared with compounds sharing common features with the polysulfonated drug. Among these are a net negative charge, position of the negative charges at both ends of the molecule, and the presence of sulfonyl or aromatic groups. One of the selected small molecules used to compare the action of suramin was brilliant blue G-250 (BBG). BBG is a disulfonated triphenylmethane known to bind polypeptides through electrostatic attraction between the negatively charged sulfonyl groups and positively charged amino acids as well as by hydrophobic interactions and heteropolar bonding with its neutral ionic species.⁸⁶ Similarly to suramin, it is characterized by a neutral central region, which corresponds to the triphenylmethane group, a distinctive structural element of the synthetic dyes, and establishes hydrophobic interactions with aromatic amino acid.⁸⁶ CD investigation showed that the stepwise addition of BBG to LL-37 dissolved in Tris buffer (Figure 6a) can trigger similar spectroscopic variations as those observed in the presence of suramin (Figure 5a, left panel),

indicating a gradual enhancement of the peptide helix content. However, a higher BBG concentration was needed to induce the peptide folding, and the much lower intensity ratio CD₂₂₂/CD₂₀₈ suggested less interacting α -helical structures. The induced aggregation is more remarkable in physiological solution (Figure S3a), where increasing the dye concentrations provoked a progressive intensity reduction of the LL-37 CD spectrum. In line with these results, DLS measurements revealed molecular assemblies on the nanometer scale in Tris buffer (Figure S4, right panel), while in PBS, the BBG addition promoted the formation of larger complex associates in the micrometer range (Figure S4, left panel). It is worth mentioning that, in the presence of suramin, larger particles were detected in both PBS and Tris buffer (Figure S2), suggesting a more effective assembly upon peptide–drug interaction. The analysis of LL-37 amide I band in Tris buffer confirmed the increase of peptide helicity resulting from the interaction with the dye molecules (Figure S5a). Moreover, it evidenced a considerable contribution from intermolecular interactions ($\sim 1682\text{ cm}^{-1}$) in PBS at a high BBG concentration (Figure S5b).

Analogously to LL-37, FK-16 also experienced a conformational change upon the stepwise addition of BBG. However, the FK-16 structure is not sensitive to the presence of inorganic anions, thus comparable results were obtained in PBS (Figure S3b) and Tris buffer (Figure S7a), where BBG induced the unordered to ordered transition of the peptide structure. In addition, light scattering measurements revealed the formation of large-sized molecular assemblies upon dye–

peptide interaction (Figure S4). These observations were supported by IR analysis, which emphasized the higher helicity for FK-16 in the complex in PBS (Figure S5c) compared to that of the precursor peptide (Figure S5b).

The cytotoxicity of LL-37 mixtures with BBG was measured on HT-29 cells (Figure 6d), where a slight increase of the IC_{50} values suggested a subtle reduction of the toxic effect at 1:1 ($15.6 \pm 4.2 \mu\text{M}$) and 1:3 ($16.9 \pm 9.1 \mu\text{M}$) peptide to dye ratios compared to that with the cathelicidin alone ($8.0 \mu\text{M} \pm 3.0$). On the contrary, the interaction with BBG did not affect the cytostatic effect of the peptide ($IC_{50} \sim 6 \mu\text{M}$).

Thereby, even though BBG was able to induce the folding of the studied peptides and formation of molecular complexes, its effect on LL-37 cytotoxicity was not comparable with the one of suramin. It should be noticed that suramin was able to induce LL-37 folding at 1:0.25 (Figure 5a, left panel) while BBG was at an 1:2.75 peptide to dye ratio (Figure 6a), which means that an ~ 11 times higher BBG concentration was needed to achieve similar conformational changes. In order to explain the weaker effect of BBG, it is important to note that, even though it contains a neutral central region, the presence of a double bond in the triphenylmethane group limits the rotation of its structure (see inset in Figure 6a). Therefore, the higher flexibility of the hydrophobic part of suramin might favor a more efficient arrangement of its structure in binding to the aromatic residues of the peptide.

In order to validate the importance of the hydrophobic central region combined with molecular flexibility, other two small molecules having therapeutic properties and carrying two negative charges were also analyzed: sulbenicillin (SBPC) and cefotetan (CTT). These latter lack a central aromatic moiety and are characterized by a 4-membered heterocyclic ring, which confers rigidity, preventing rotation of the chemical structure. The α -sulfo-benzyl penicillin (SBPC) is a negatively charged β -lactam with a sulfonic group and, in physiological conditions, carries two negative charges located at both extremities. CD curves displayed slight variations of the LL-37 secondary structure upon interaction with SBPC (1:1 and 1:6 peptide to drug ratios), namely, a red shift of the negative band at ~ 200 nm, which also decreases in intensity while the shoulder at ~ 227 nm becomes more pronounced (Figure 6b). Moreover, large-sized particles in the micrometer range were detected in the presence of SBPC (Figure S6, left panel), suggesting peptide interaction and assembly formation. The observed spectral changes indicated that the interaction with the negatively charged antibiotic might moderately raise the peptide α -helix content without, however, altering its cytotoxic and cytostatic activity (Figure 6e). Similar spectral changes were induced by CTT, a cephalosporin bearing two negative charges with a cephem skeleton and lacking sulfonic groups, starting from an 1:4 peptide to drug ratio (Figure 6c). Analogously to SBPC, also, CTT induced formation of the assemblies (Figure S6, right panel), but, just as with SBPC, CTT could not prevent LL-37 toxicity at the studied concentrations (Figure 6f). FK-16 conformation was less affected by the interaction with the studied antibiotics; indeed, no significant change of the CD profile can be observed (Figure S7b,c). However, a significant reduction of the spectral intensity occurred, suggesting an association of the peptide chains. In accordance with CD data, DLS measurements (Figure S6) revealed the formation of peptide–drug assemblies on the micrometer scale, in a similar way to that of the full-length peptide.

Thereby, even though SBPC and CTT were demonstrated to interact with LL-37, the structure of the peptide was only moderately affected and its toxicity to mammalian cells was not significantly prevented. These data pointed out the critical role of the hydrophobic moiety, a characteristic of suramin and BBG, for driving the peptide folding. Indeed, besides the highly polyanionic nature of suramin, other structural features might be crucial for performing its action. Its symmetric structure contains rotatable bonds, and it is characterized by two terminal naphthyl rings with a bridging central part. Both terminal regions carry charged sulfonate groups on the naphthalene rings beside the amide bonds, while its central portion is neutral. According to computational studies,⁸⁷ the free energy contribution of the neutral central part (Figure 1c) is crucial for the binding with the hydrophobic moieties of a peptide through van der Waals interactions. Therefore, even if electrostatic attractions play a key role in charge neutralization and the formation of drug–peptide complexes, hydrophobic interactions could significantly contribute to alter the peptide structure and its ability to interact with mammalian cells. Nevertheless, the importance is the peculiar structural flexibility of suramin, whose rotatable bonds might optimize the binding to the peptide and play a pivotal role in the reduction of the cytotoxic effect of the cathelicidin.

Moreover, the sequential preference of suramin for the peptide partner LL-37 should be considered, as well as the 37 amino acid long sequence, which may offer several binding places for the drug. In this respect, the analogous suramin–peptide measurements with FK-16 were rather informative, as the two peptides showed similar behavior during cytotoxicity, internalization, and conformational changes even in the presence of the other tested drug molecules. Consequently, it is proposed that the corresponding 16-residue sequence is directly involved in the suramin–LL-37 interactions.

CONCLUSIONS

In this study, we have shown that the multipurpose drug suramin was able to reduce cellular internalization and the consequent toxic effect of the cathelicidin peptide LL-37 on the viability and growth of colon and monocytic cell lines. Molecular insights of this action were obtained from the combination of different spectroscopic methods, which indicated folding of the peptide secondary structure upon interaction with suramin and formation of drug–peptide complexes. On the basis of analogous measurements with FK-16, it is strongly suggested that the corresponding sequential region of LL-37 most likely binds suramin with high affinity. The investigation of peptide interaction with other negatively charged small molecules with peculiar structural elements suggested that the unique action exerted by suramin might be related not only to its polyanionic nature but also to the presence of a hydrophobic central part and rotatable bonds. It is possible to assume that these molecular features enable the drug to optimize the interaction with the peptide chain, leading to the formation of complexes in which the binding of the peptide to cell surfaces and receptors is prevented.

This new action of suramin on LL-37 cytotoxicity could potentially be exploited for novel repurposing strategies aimed to prevent inflammatory responses occurring in several disorders as a consequence of the cathelicidin dysregulated overexpression. Considering peptide hormones, and other host defense peptides with regulatory functions, we hope that the current results will promote studies aiming to find further

drugs with similar complexing capacities. This may not only provide new strategies for controlling various dysregulations but also could result in better mapping of *in vivo* interactions of these compounds. Note, however, that a significant amount of further investigations, such as in depth studies on *in vivo* systems focusing on specific autoimmune and inflammatory diseases, is clearly needed in order to properly evaluate the practical benefits of the present approach and to reach an appropriate comparison with the currently established treatments.

METHODS

Materials. LL-37 and FK-16 were synthesized by NovoPro Bioscience Inc. (Shanghai, China). The molecular mass (MW) of the peptides was determined by mass spectroscopy. For LL-37 (MW = 4492.8), the peptide purity corresponded to 96.6% and the net peptide content was 72.1%. In the case of FK-16 (MW = 2044.4), the peptide purity was 95.1% and the net peptide content was 72.0%. For the preparation of peptide solutions, lyophilized powders were dissolved in high-purity water at a concentration not higher than 1 mM, and the mixture was aliquoted and stored at -18°C . Suramin sodium salt $\geq 99\%$ (TLC) (S2671) was purchased from Sigma-Aldrich (Budapest, Hungary). Brilliant Blue G-250 $\geq 95\%$ (AC191480050, Reanal Labor) was obtained from Acros Organics (Geel, Belgium). Cefotetan disodium salt $\geq 95\%$ (GA5476, Glentham Life Science) and sulbenicillin sodium $\geq 98\%$ (BD152125, BLDpharm) were purchased from ChemPur (Karlsruhe, Germany). The solutions were prepared by dissolving the compound powder in high-purity water at a concentration not higher than 1 mM, and the mixtures were aliquoted and stored at -18°C . For the cellular uptake studies, peptides labeled with 5(6)-carboxyfluorescein (Cf) on the N-terminus (purity $\geq 95\%$) were purchased from NovoPro Bioscience Inc. (Shanghai, China). As one dye molecule was coupled to each peptide, the fluorescence properties and the cellular uptake values are comparable. Previous investigation on a set of representative peptides⁸⁸ demonstrated that the Cf labeling did not modify the tendency compared with those of unlabeled peptides in case of internalization rate as a consequence of altered lipophilicity and charge.

Cell Culturing and Cytotoxicity/Cytostasis Assays. MonoMac6 human monocytic cell line⁸⁹ (DSMZ no.: ACC 124) was cultured in complete medium prepared from RPMI-1640 (Lonza, Basel, Switzerland) supplemented with 10% heat-inactivated fetal calf serum (FCS, Lonza), 2 mM L-glutamine (Lonza), and 160 $\mu\text{g}/\text{mL}$ gentamycin (Sigma-Aldrich, Budapest, Hungary) at 37°C in a 5% CO_2 atmosphere. HT-29 human colon adenocarcinoma cells⁹⁰ (ATCC:HTB-38) were maintained in RPMI-1640, supplied with 10% FCS, L-glutamine, and 1% penicillin–streptomycin (from 10 000 units penicillin and 10 mg streptomycin/mL, Gibco, Dublin, Ireland), and under the conditions described above. No mycoplasma contamination was detected in the cell cultures.

For cytotoxicity assay, cells were distributed on a 96-well flat bottom tissue culture plate (Sarstedt, Nümbrecht, Germany) (15 000 MonoMac6 cells/100 μL /well or 10 000 HT-29 cells/100 μL /well in complete RPMI-1640 medium).

Peptides and small molecules to be tested were dissolved in serum-free medium (SFM) and added to the cells to achieve final concentrations of 0.02–33 μM for LL-37 and 0.05–100

μM for FK-16. Cells were incubated with the peptides for 4 h and then washed three times with SFM.

The cell viability was tested using MTT assay^{91–93} for MonoMac6 cells and Alamar Blue for HT-29 cells. Briefly, 45 μL of MTT (3-(4,5-dimethylthiazol-2-yl)-2,5-diphenyltetrazolium bromide, Sigma-Aldrich, Budapest, Hungary) solutions (2 mg/mL, in SFM) was added to each well, followed by 4 h of incubation, and plates were centrifuged at 2000 rpm for 5 min, and the supernatant was carefully removed. The purple formazan crystals were dissolved in 100 μL of DMSO, and after 10 min of agitation, the absorbance was determined at $\lambda = 540$ and 620 nm using an ELISA plate reader (iEMS Reader, Labsystems, Vantaa, Finland). For Alamar Blue assay, 20 μL of Alamar Blue (resazurin sodium salt, Sigma-Aldrich, Budapest, Hungary) solution (0.15 mg/mL, dissolved in PBS, pH 7.4) was added to each well. Following a 4 h incubation, the fluorescence was measured using a Synergy H4 multimode microplate reader (BioTek, Winooski, VT) ($\lambda_{\text{Ex}} = 530/30$ and $\lambda_{\text{Em}} = 610/10$ nm).

To determine the cytostatic effect, 5000 cells per well were plated in 96-well flat bottom tissue culture plates (Sarstedt, Nümbrecht, Germany) in RPMI-1640 complete medium. After 24 h, the cells were treated with the peptides and small molecules in SFM (concentration range 0.02–100 μM). After overnight incubation, the cells were washed three times with SFM and cultured for 72 h in complete medium. The cell viability was determined using MTT or Alamar Blue assays, according to the cell line.

All measurements were performed in triplicate, and the mean IC_{50} values together with SEM were represented in the graphs.

Cell Morphology. To visualize the cell morphology after peptide treatment, microscopic images of HT-29 cells were captured. HT-29 cells were plated in a 96-well flat bottom tissue culture plate (5000 cells/100 μL of RPMI-1640 medium without phenol red) and then treated with the peptides for 1.5 h at 17 μM LL-37 and 33 μM FK-16 alone and in combination with suramin. Microscopic images of the adherent cells were captured using an Olympus CKX41 microscope (Hamburg, Germany, equipped with an Olympus U-RFLT50 mercury-vapor lamp, WideBlue DMS500 BP460-490 BA520 IF filter; excitation wavelength range, 460–490 nm; objective, 20 \times).

Cellular Uptake Evaluation by Flow Cytometry. The cellular uptake of Cf-labeled LL-37 and FK-16 with suramin was studied on HT-29 cells. The cells were seeded in a 24-well tissue culture plate (5000 cells/well, Sarstedt, Nümbrecht, Germany) in complete medium. On the next day, the cells were treated with Cf-peptides and suramin (at 10, 5, and 1 μM final concentrations) in SFM. After 1.5 h, the cells were washed once with SFM and once with HPMI medium (9 mM glucose, 10 mM NaHCO_3 , 119 mM NaCl, 9 mM HEPES, 5 mM KCl, 0.85 mM MgCl_2 , 0.053 mM CaCl_2 , 5 mM $\text{Na}_2\text{HPO}_4 \cdot 2\text{H}_2\text{O}$, pH 7.4 was prepared in-house using components obtained from Sigma-Aldrich, Budapest, Hungary) and detached with trypsin (Sigma-Aldrich, Budapest, Hungary) for 10 min at 37°C . Trypsin was then inactivated using 10% FCS/HPMI, and cells were centrifuged at 1000 rpm for 5 min at 4°C . Afterward, the supernatant was removed, and the cells were resuspended in HPMI medium. To detect the intracellular fluorescence intensity, which is proportional to the cellular uptake, cell suspensions were analyzed by a BD LSR II flow cytometer (BD Bioscience, San Jose, CA) equipped with a 488 nm (22 mW, Coherent Sapphire, Santa Clara, CA) laser

(channel FITC LP505; emission at $\lambda = 505$ nm; LP 505, BP 530/30; forward and side scattered (FSC, SSC)) light intensity. Obtained data were analyzed by FACSDiVa (BD Bioscience, San Jose, CA) 5.0 software. All measurements were performed in triplicate, and the mean fluorescent intensity and the percentage of FITC positive cells were presented.

Confocal Microscopy. HT-29 cells were seeded to coverslip-containing (thickness 1, Assistant, Karl Hecht GmbH & Co KG, Sondheim/Rhön, Germany) 24-well tissue culture plates 1 day prior to sample preparation (10^5 cells/well). Lysosomes were stained with LysoTracker Deep Red (Thermo Fisher Scientific, Bremen, Germany, 30 min, according to the manufacturer's instructions), which was followed by treatment with Cf-labeled peptide (LL-37, dissolved in SFM, $1 \mu\text{M}$ final concentration, 1.5 h) with or without the addition of suramin (0.5 or $2 \mu\text{M}$). As a control, suramin was also used separately ($2 \mu\text{M}$). Nuclei were stained with Hoechst 33342 ($0.5 \mu\text{g/mL}$, 10 min, Thermo Fisher Scientific, Bremen, Germany). Cells were fixed with 4% paraformaldehyde (15 min, Sigma-Aldrich, Budapest, Hungary), and samples were mounted to microscopy slides (VWR) using Mowiol 4-88 mounting medium (Sigma-Aldrich, Budapest, Hungary). Imaging was performed on a Zeiss LSM 710 system (Carl Zeiss Microscopy GmbH, Jena, Germany) with a $40\times$ oil objective using the following parameters: Cf-labeled peptide $\lambda_{\text{ex}} = 488$ nm, $\lambda_{\text{em}} = 541$ nm, nuclei $\lambda_{\text{ex}} = 405$ nm, $\lambda_{\text{em}} = 467$ nm (Hoechst 33342), lysosomes $\lambda_{\text{ex}} = 633$ nm, $\lambda_{\text{em}} = 720$ nm (LysoTracker). Zeiss ZEN lite software (Carl Zeiss Microscopy GmbH, Jena, Germany) was used for image processing.

Circular Dichroism (CD) Spectroscopy. CD measurements were performed using a JASCO J-1500 spectropolarimeter at ambient temperature in a 0.1 cm path length cylindrical quartz cuvette (Hellma, Plainview, NY). CD spectra were collected in continuous scanning mode between 190 and 260 nm at a rate of 50 nm min^{-1} , 1 nm bandwidth, step size of 0.5 nm , and a response time of 4 s, for 3 accumulations. CD curves of peptide, peptide/suramin, and peptide/dye were corrected by the contribution of a matching blank. The peptide secondary structure content was estimated using the software BeStSel (Beta Structure Selection, <http://bestsel.elte.hu>).⁹⁴

Attenuated Total Reflection Fourier-Transform Infrared (ATR-FTIR) Spectroscopy. ATR-FTIR measurements were carried out using a Varian 2000 FTIR Scimitar Series spectrometer (Varian Inc., Palo Alto, CA) equipped with a liquid nitrogen cooled mercury–cadmium–telluride (MCT) detector and with a “Golden Gate” single reflection diamond ATR accessory (Specac Ltd., Orpington, UK). The sample ($5 \mu\text{L}$) was mounted onto the diamond ATR crystal, and spectra were acquired after slow evaporation of the buffer solvent (within approximately 15 min) under ambient conditions, at a nominal resolution of 2 cm^2 and coadding 64 scans. Each data acquisition was followed by ATR correction, and the spectra were smoothed by applying the Savitzky-Golay algorithm. Buffer subtraction and baseline correction were also performed. For the second derivative analysis, spectra were normalized by the area. Spectra analysis was carried out using Origin software package (OriginLab, Northampton, MA).

Dynamic Light Scattering (DLS). Samples were measured with a W130i dynamic light scattering device (DLS, Avid Nano, Ltd., High Wycombe, UK) with a diode laser (660 nm) and a photodiode detector, using low-volume disposable cuvettes with 1 cm path length (UVette, Eppendorf, Vienna,

Austria, GmbH). The autocorrelations functions were measured for 10 s, repeated 10 times, and analyzed with the supplied iSize 3.0 software.

■ ASSOCIATED CONTENT

Supporting Information

The Supporting Information is available free of charge at <https://pubs.acs.org/doi/10.1021/acspsci.0c00155>.

Figures of cytotoxicity effect of LL-37 and FK-16 on MonoMac6 cells, DLS investigations, far-UV spectra, peptide spectra, monitoring aggregate formation in the presence of antibiotics, and far-UV CD spectra (PDF)

■ AUTHOR INFORMATION

Corresponding Author

Tamás Beke-Somfai – *Institute of Materials and Environmental Chemistry, Research Centre for Natural Sciences, Biomolecular Self-Assembly Research Group, Budapest H-1117, Hungary; Phone: +36 1 3826 689; Email: beke-somfai.tamas@ttk.mta.hu*

Authors

Mayra Quemé-Peña – *Institute of Materials and Environmental Chemistry, Research Centre for Natural Sciences, Biomolecular Self-Assembly Research Group, Budapest H-1117, Hungary; Institute of Chemistry, Eötvös Loránd University, Budapest H-1117, Hungary;*

orcid.org/0000-0002-0257-6594

Maria Ricci – *Institute of Materials and Environmental Chemistry, Research Centre for Natural Sciences, Biomolecular Self-Assembly Research Group, Budapest H-1117, Hungary;*

orcid.org/0000-0002-8548-5427

Tünde Juhász – *Institute of Materials and Environmental Chemistry, Research Centre for Natural Sciences, Biomolecular Self-Assembly Research Group, Budapest H-1117, Hungary*

Kata Horváti – *MTA-ELTE Research Group of Peptide Chemistry, Eötvös Loránd University, Hungarian Academy of Sciences, Budapest H-1117, Hungary; Institute of Chemistry, Eötvös Loránd University, Budapest H-1117, Hungary;*

orcid.org/0000-0003-4092-6011

Szilvia Bősze – *MTA-ELTE Research Group of Peptide Chemistry, Eötvös Loránd University, Hungarian Academy of Sciences, Budapest H-1117, Hungary;*

orcid.org/0000-0001-9555-699X

Beáta Biri-Kovács – *MTA-ELTE Research Group of Peptide Chemistry, Eötvös Loránd University, Hungarian Academy of Sciences, Budapest H-1117, Hungary; Institute of Chemistry, Eötvös Loránd University, Budapest H-1117, Hungary*

Bálint Szeder – *Institute of Enzymology, Research Centre for Natural Sciences, Budapest H-1117, Hungary*

Ferenc Zsila – *Institute of Materials and Environmental Chemistry, Research Centre for Natural Sciences, Biomolecular Self-Assembly Research Group, Budapest H-1117, Hungary;*

orcid.org/0000-0002-4853-2810

Complete contact information is available at:

<https://pubs.acs.org/doi/10.1021/acspsci.0c00155>

Notes

The authors declare no competing financial interest.

ACKNOWLEDGMENTS

This study was financially supported by the Momentum Program (LP2016-2), the National Competitiveness and Excellence Program (NVKP_16-1-2016-0007), and the BIONANO_GINOP-2.3.2-15-2016-00017 project. S.B., B.B.-K., and K.H. would like to thank the ELTE Institutional Excellence Program (NKFIH-1157-8/2019-DT), the Hungarian Ministry of Human Capacities, the ELTE Thematic Excellence Programme (Szint+), and the Hungarian Ministry for Innovation and Technology. The work was also supported by the National Research, Development and Innovation Fund of Hungary (2018-1.2.1-NKP-2018-00005). K.H. was supported by the Premium Post-Doctoral Fellowship of the Hungarian Academy of Sciences.

REFERENCES

- (1) Van Harten, R. M., Van Woudenberg, E., Van Dijk, A., and Haagsman, H. P. (2018) Cathelicidins: Immunomodulatory Antimicrobials. *Vaccines* 6, 63.
- (2) Hilchie, A. L., Wuerth, K., and Hancock, R. E. W. (2013) Immune modulation by multifaceted cationic host defense (antimicrobial) peptides. *Nat. Chem. Biol.* 9, 761–768.
- (3) Kai-Larsen, Y., and Agerberth, B. (2008) The role of the multifunctional peptide LL-37 in host defense. *Front. Biosci., Landmark Ed.* 13, 3760–3767.
- (4) Verjans, E.-T., Zels, S., Luyten, W., Landuyt, B., and Schoofs, L. (2016) Molecular mechanisms of LL-37-induced receptor activation: An overview. *Peptides* 85, 16–26.
- (5) Chieosilapatham, P., Ikeda, S., Ogawa, H., and Niyonsaba, F. (2018) Tissue-specific regulation of innate immune responses by human cathelicidin LL-37. *Curr. Pharm. Des.* 24, 1079–1091.
- (6) Kuroda, K., Okumura, K., Isogai, H., and Isogai, E. (2015) The Human Cathelicidin Antimicrobial Peptide LL-37 and Mimics are Potential Anticancer Drugs. *Front. Oncol.* 5, 144.
- (7) Wang, G., Narayana, J. L., Mishra, B., Zhang, Y., Wang, F., Wang, C., Zarena, D., Lushnikova, T., and Wang, X. (2019) Design of Antimicrobial Peptides: Progress Made with Human Cathelicidin LL-37, in *Antimicrobial Peptides: Basics for Clinical Application* (Matsuzaki, K., Ed.) pp 215–240, Springer, Singapore.
- (8) Vandamme, D., Landuyt, B., Luyten, W., and Schoofs, L. (2012) A comprehensive summary of LL-37, the factotum human cathelicidin peptide. *Cell. Immunol.* 280, 22–35.
- (9) Sorensen, O. E., Follin, P., Johnsen, A. H., Calafat, J., Tjabringa, G. S., Hiemstra, P. S., and Borregaard, N. (2001) Human cathelicidin, hCAP-18, is processed to the antimicrobial peptide LL-37 by extracellular cleavage with proteinase 3. *Blood* 97, 3951–3959.
- (10) Sun, M., He, C., Cong, Y., and Liu, Z. (2015) Regulatory immune cells in regulation of intestinal inflammatory response to microbiota. *Mucosal Immunol.* 8, 969–978.
- (11) Schaubert, J., Svanholm, C., Termén, S., Iffland, K., Menzel, T., Scheppach, W., Melcher, R., Agerberth, B., Lührs, H., and Gudmundsson, G. H. (2003) Expression of the cathelicidin LL-37 is modulated by short chain fatty acids in colonocytes: relevance of signalling pathways. *Gut* 52, 735–741.
- (12) O’Neil, D. A., Porter, E. M., Elewaut, D., Anderson, G. M., Eckmann, L., Ganz, T., and Kagnoff, M. F. (1999) Expression and Regulation of the Human β -Defensins hBD-1 and hBD-2 in Intestinal Epithelium. *J. Immunol.* 163, 6718–6724.
- (13) Dürr, U. H. N., Sudheendra, U. S., and Ramamoorthy, A. (2006) LL-37, the only human member of the cathelicidin family of antimicrobial peptides. *Biochim. Biophys. Acta, Biomembr.* 1758, 1408–1425.
- (14) Xhindoli, D., Pacor, S., Benincasa, M., Scocchi, M., Gennaro, R., and Tossi, A. (2016) The human cathelicidin LL-37 — A pore-forming antibacterial peptide and host-cell modulator. *Biochim. Biophys. Acta, Biomembr.* 1858, 546–566.
- (15) Turner, J., Cho, Y., Dinh, N.-N., Waring, A. J., and Lehrer, R. I. (1998) Activities of LL-37, a Cathelin-Associated Antimicrobial Peptide of Human Neutrophils. *Antimicrob. Agents Chemother.* 42, 2206–2214.
- (16) Bowdish, D. M. E., Davidson, D. J., Speert, D. P., and Hancock, R. E. W. (2004) The Human Cationic Peptide LL-37 Induces Activation of the Extracellular Signal-Regulated Kinase and p38 Kinase Pathways in Primary Human Monocytes. *J. Immunol.* 172, 3758–3765.
- (17) Agerberth, B., Charo, J., Werr, J., Olsson, B., Idali, F., Lindbom, L., Kiessling, R., Jörnvall, H., Wigzell, H., and Gudmundsson, G. H. (2000) The human antimicrobial and chemotactic peptides LL-37 and α -defensins are expressed by specific lymphocyte and monocyte populations. *Blood* 96, 3086–3093.
- (18) Larrick, J. W., Hirata, M., Balint, R. F., Lee, J., Zhong, J., and Wright, S. C. (1995) Human CAP18: a novel antimicrobial lipopolysaccharide-binding protein. *Infect. Immun.* 63, 1291–1297.
- (19) Henzler-Wildman, K. A., Martinez, G. V., Brown, M. F., and Ramamoorthy, A. (2004) Perturbation of the Hydrophobic Core of Lipid Bilayers by the Human Antimicrobial Peptide LL-37. *Biochemistry* 43, 8459–8469.
- (20) Burton, M. F., and Steel, P. G. (2009) The chemistry and biology of LL-37. *Nat. Prod. Rep.* 26, 1572–1584.
- (21) Girmita, A., Zheng, H., Grönberg, A., Girmita, L., and Ståhle, M. (2012) Identification of the cathelicidin peptide LL-37 as agonist for the type I insulin-like growth factor receptor. *Oncogene* 31, 352–365.
- (22) Tomasiński, L., Pizzirani, C., Skerlavaj, B., Pellegatti, P., Gulinelli, S., Tossi, A., Virgilio, F. D., and Zanetti, M. (2008) The Human Cathelicidin LL-37 Modulates the Activities of the P2X₇ Receptor in a Structure-dependent Manner. *J. Biol. Chem.* 283, 30471–30481.
- (23) Ciornei, C. D., Sigurdardóttir, T., Schmidtchen, A., and Bodelsson, M. (2005) Antimicrobial and Chemoattractant Activity, Lipopolysaccharide Neutralization, Cytotoxicity, and Inhibition by Serum of Analogs of Human Cathelicidin LL-37. *Antimicrob. Agents Chemother.* 49, 2845–2850.
- (24) Säll, J., Carlsson, M., Gidlöf, O., Holm, A., Humlén, J., Öhman, J., Svensson, D., Nilsson, B.-O., and Jönsson, D. (2013) The Antimicrobial Peptide LL-37 Alters Human Osteoblast Ca²⁺ Handling and Induces Ca²⁺-Independent Apoptosis. *J. Innate Immun.* 5, 290–300.
- (25) Ciornei, C. D., Tapper, H., Bjartell, A., Sternby, N. H., and Bodelsson, M. (2006) Human antimicrobial peptide LL-37 is present in atherosclerotic plaques and induces death of vascular smooth muscle cells: a laboratory study. *BMC Cardiovasc. Disord.* 6, 49.
- (26) Zhang, Z., Cherryholmes, G., and Shively, J. E. (2008) Neutrophil secondary necrosis is induced by LL-37 derived from cathelicidin. *J. Leukocyte Biol.* 84, 780–788.
- (27) Barlow, P. G., Beaumont, P. E., Cosseau, C., Mackellar, A., Wilkinson, T. S., Hancock, R. E. W., Haslett, C., Govan, J. R. W., Simpson, A. J., and Davidson, D. J. (2010) The Human Cathelicidin LL-37 Preferentially Promotes Apoptosis of Infected Airway Epithelium. *Am. J. Respir. Cell Mol. Biol.* 43, 692–702.
- (28) Mader, J. S., Ewen, C., Hancock, R. E. W., and Bleackley, R. C. (2011) The Human Cathelicidin, LL-37, Induces Granzyme-mediated Apoptosis in Regulatory T Cells. *J. Immunother.* 34, 229–235.
- (29) Frasca, L., and Lande, R. (2012) Role of defensins and cathelicidin LL37 in auto-immune and auto-inflammatory diseases. *Curr. Pharm. Biotechnol.* 13, 1882–1897.
- (30) Kahlenberg, J. M., and Kaplan, M. J. (2013) Little Peptide, Big Effects: The Role of LL-37 in Inflammation and Autoimmune Disease. *J. Immunol.* 191, 4895–4901.
- (31) Garcia-Romo, G. S., Caielli, S., Vega, B., Connolly, J., Allantaz, F., Xu, Z., Punaro, M., Baisch, J., Guiducci, C., Coffman, R. L., Barrat, F. J., Banchereau, J., and Pascual, V. (2011) Netting Neutrophils Are Major Inducers of Type I IFN Production in Pediatric Systemic Lupus Erythematosus. *Sci. Transl. Med.* 3, 73ra20–73ra20.
- (32) Paulsen, F., Pufe, T., Conradi, L., Varoga, D., Tsokos, M., Papendieck, J., and Petersen, W. (2002) Antimicrobial peptides are

expressed and produced in healthy and inflamed human synovial membranes. *J. Pathol.* 198, 369–377.

(33) Albanesi, C. (2019) 64 - Immunology of Psoriasis, in *Clinical Immunology* (Rich, R. R., Fleisher, T. A., Shearer, W. T., Schroeder, H. W., Frew, A. J., and Weyand, C. M., Eds.) Fifth ed., pp 871–878.e1, Elsevier, London, UK.

(34) Reinholz, M., Ruzicka, T., and Schaubert, J. (2012) Cathelicidin LL-37: An Antimicrobial Peptide with a Role in Inflammatory Skin Disease. *Ann. Dermatol.* 24, 126–135.

(35) Kulkarni, N. N., Takahashi, T., Sanford, J. A., Tong, Y., Gombart, A. F., Hinds, B., Cheng, J. Y., and Gallo, R. L. (2020) Innate Immune Dysfunction in Rosacea Promotes Photosensitivity and Vascular Adhesion Molecule Expression. *J. Invest. Dermatol.* 140, 645–655.

(36) Salzer, S., Kresse, S., Hirai, Y., Koglin, S., Reinholz, M., Ruzicka, T., and Schaubert, J. (2014) Cathelicidin peptide LL-37 increases UVB-triggered inflammasome activation: Possible implications for rosacea. *J. Dermatol. Sci.* 76, 173–179.

(37) Kusaka, S., Nishida, A., Takahashi, K., Bamba, S., Yasui, H., Kawahara, M., Inatomi, O., Sugimoto, M., and Andoh, A. (2018) Expression of human cathelicidin peptide LL-37 in inflammatory bowel disease. *Clin. Exp. Immunol.* 191, 96–106.

(38) Sun, L., Wang, W., Xiao, W., and Yang, H. (2016) The Roles of Cathelicidin LL-37 in Inflammatory Bowel Disease. *Inflamm. Bowel Dis.* 22, 1986–1991.

(39) Schaubert, J., Rieger, D., Weiler, F., Wehkamp, J., Eck, M., Fellermann, K., Scheppach, W., Gallo, R. L., and Stange, E. F. (2006) Heterogeneous expression of human cathelicidin hCAP18/LL-37 in inflammatory bowel diseases. *Eur. J. Gastroenterol. Hepatol.* 18, 615–621.

(40) Gutiérrez, A., Holler, E., Zapater, P., Sempere, L., Jover, R., Pérez-Mateo, M., Schoelmerich, J., Such, J., Wiest, R., and Francés, R. (2011) Antimicrobial peptide response to blood translocation of bacterial DNA in Crohn's disease is affected by NOD2/CARD15 genotype. *Inflamm. Bowel Dis.* 17, 1641–1650.

(41) Agier, J., Efenberger, M., and Brzezińska-Błaszczak, E. (2015) Review paper Cathelicidin impact on inflammatory cells. *Cent. Eur. J. Immunol.* 2, 225–235.

(42) Svensson, D., Lagerstedt, J. O., Nilsson, B.-O., and Del Giudice, R. (2017) Apolipoprotein A-I attenuates LL-37-induced endothelial cell cytotoxicity. *Biochem. Biophys. Res. Commun.* 493, 71–76.

(43) Wang, Y., Johansson, J., Agerberth, B., Jörnvall, H., and Griffiths, W. J. (2004) The antimicrobial peptide LL-37 binds to the human plasma protein apolipoprotein A-I. *Rapid Commun. Mass Spectrom.* 18, 588–589.

(44) Felgentreff, K., Beisswenger, C., Griese, M., Gulder, T., Bringmann, G., and Bals, R. (2006) The antimicrobial peptide cathelicidin interacts with airway mucus. *Peptides* 27, 3100–3106.

(45) Zhang, X., Bajic, G., Andersen, G. R., Christiansen, S. H., and Vorup-Jensen, T. (2016) The cationic peptide LL-37 binds Mac-1 (CD11b/CD18) with a low dissociation rate and promotes phagocytosis. *Biochim. Biophys. Acta, Proteins Proteomics* 1864, 471–478.

(46) Zsila, F., Kohut, G., and Beke-Somfai, T. (2019) Disorder-to-helix conformational conversion of the human immunomodulatory peptide LL-37 induced by antiinflammatory drugs, food dyes and some metabolites. *Int. J. Biol. Macromol.* 129, 50–60.

(47) Wiedemar, N., Hauser, D. A., and Mäser, P. (2020) 100 Years of Suramin. *Antimicrob. Agents Chemother.* 64, e01168.

(48) Quemé-Peña, M., Juhász, T., Mihály, J., Cs. Szgyártó, I., Horváti, K., Bősze, S., Henczkó, J., Pályi, B., Németh, C., Varga, Z., Zsila, F., and Beke-Somfai, T. (2019) Manipulating Active Structure and Function of Cationic Antimicrobial Peptide CM15 with the Polysulfonated Drug Suramin: A Step Closer to in Vivo Complexity. *ChemBioChem* 20, 1578–1590.

(49) Hawking, F. (1978) Suramin: With Special Reference to Onchocerciasis. *Adv. Pharmacol. Chemother.* 15, 289–322.

(50) Wainwright, M. (2010) Dyes, trypanosomiasis and DNA: a historical and critical review. *Biotech. Histochem.* 85, 341–354.

(51) Fernández-Prada, C., Douanne, N., Minguez-Menendez, A., Pena, J., Tunes, L. G., Pires, D. E. V., and Monte-Neto, R. L. (2019) Chapter 5 - Repurposed Molecules: A New Hope in Tackling Neglected Infectious Diseases, in *In Silico Drug Design* (Roy, K., Ed.) pp 119–160, Academic Press.

(52) Henß, L., Beck, S., Weidner, T., Biedenkopf, N., Sliva, K., Weber, C., Becker, S., and Schnierle, B. S. (2016) Suramin is a potent inhibitor of Chikungunya and Ebola virus cell entry. *Virology* 13, 149.

(53) Chen, Y., Maguire, T., Hileman, R. E., Fromm, J. R., Esko, J. D., Linhardt, R. J., and Marks, R. M. (1997) Dengue virus infectivity depends on envelope protein binding to target cell heparan sulfate. *Nat. Med.* 3, 866–871.

(54) Cheng, B., Gao, F., Maissy, E., and Xu, P. (2019) Repurposing suramin for the treatment of breast cancer lung metastasis with glycol chitosan-based nanoparticles. *Acta Biomater.* 84, 378–390.

(55) Mirza, M. R., Jakobsen, E., Pfeiffer, P., Lindebjerg-Clasen, B., Bergh, J., and Rose, C. (1997) Suramin in Non-small Cell Lung Cancer and Advanced Breast Cancer: Two Parallel Phase II Studies. *Acta Oncol.* 36, 171–174.

(56) Ord, J. J., Streeter, E., Jones, A., Monnier, K. L., Cranston, D., Crew, J., Joel, S. P., Rogers, M. A., Banks, R. E., Roberts, I. S. D., and Harris, A. L. (2005) Phase I trial of intravesical Suramin in recurrent superficial transitional cell bladder carcinoma. *Br. J. Cancer* 92, 2140–2147.

(57) Bhargava, S., Hotz, B., Hines, O. J., Reber, H. A., Buhr, H. J., and Hotz, H. G. (2007) Suramin Inhibits Not Only Tumor Growth and Metastasis but Also Angiogenesis in Experimental Pancreatic Cancer. *J. Gastrointest. Surg.* 11, 171–178.

(58) Naviaux, R. K., Curtis, B., Li, K., Naviaux, J. C., Bright, A. T., Reiner, G. E., Westerfield, M., Goh, S., Alaynick, W. A., Wang, L., Capparelli, E. V., Adams, C., Sun, J., Jain, S., He, F., Arellano, D. A., Mash, L. E., Chukoskie, L., Lincoln, A., and Townsend, J. (2017) Low-dose suramin in autism spectrum disorder: a small, phase I/II, randomized clinical trial. *Ann. Clin. Transl. Neurol.* 4, 491–505.

(59) Naviaux, J. C., Schuchbauer, M. A., Li, K., Wang, L., Risbrough, V. B., Powell, S. B., and Naviaux, R. K. (2014) Reversal of autism-like behaviors and metabolism in adult mice with single-dose antipurinergic therapy. *Transl. Psychiatry* 4, e400–e400.

(60) Hamidpour, R., Hamidpour, S., Hamidpour, M., Zarabi, M. H., Sohraby, M., and Shalari, M. (2016) Antipurinergic Therapy with Suramin as a Treatment for Autism Spectrum Disorder. *J. Biomedical Sci.* 5, 1.

(61) Li, X., Li, Y., Han, H., Miller, D. W., and Wang, G. (2006) Solution structures of human LL-37 fragments and NMR-based identification of a minimal membrane-targeting antimicrobial and anticancer region. *J. Am. Chem. Soc.* 128, 5776–5785.

(62) Ren, S. X., Shen, J., Cheng, A. S. L., Lu, L., Chan, R. L. Y., Li, Z. J., Wang, X. J., Wong, C. C. M., Zhang, L., Ng, S. S. M., Chan, F. L., Chan, F. K. L., Yu, J., Sung, J. J. Y., Wu, W. K. K., Cho, C. H., and Nie, D. (2013) FK-16 Derived from the Anticancer Peptide LL-37 Induces Caspase-Independent Apoptosis and Autophagic Cell Death in Colon Cancer Cells. *PLoS ONE* 8, e63641.

(63) Chan, C.-F., and Lin-Shiau, S.-Y. (2001) Suramin prevents cerebellar granule cell-death induced by dequalinium. *Neurochem. Int.* 38, 135–143.

(64) Jiang, L.-H., Mackenzie, A. B., North, R. A., and Surprenant, A. (2000) Brilliant Blue G Selectively Blocks ATP-Gated Rat P2 × 7 Receptors. *Mol. Pharmacol.* 58, 82–88.

(65) Jo, S., and Bean, B. P. (2011) Inhibition of Neuronal Voltage-Gated Sodium Channels by Brilliant Blue G. *Mol. Pharmacol.* 80, 247–257.

(66) Ryu, J. K., and McLarnon, J. G. (2008) Block of purinergic P2 × 7 receptor is neuroprotective in an animal model of Alzheimer's disease. *NeuroReport* 19, 1715–1719.

(67) Díaz-Hernández, M., Díez-Zaera, M., Sánchez-Nogueiro, J., Gómez-Villafuertes, R., Canals, J. M., Alberch, J., Miras-Portugal, M. T., and Lucas, J. J. (2009) Altered P2 × 7-receptor level and function in mouse models of Huntington's disease and therapeutic efficacy of antagonist administration. *FASEB J.* 23, 1893–1906.

- (68) Peng, W., Cotrina, M. L., Han, X., Yu, H., Bekar, L., Blum, L., Takano, T., Tian, G.-F., Goldman, S. A., and Nedergaard, M. (2009) Systemic administration of an antagonist of the ATP-sensitive receptor P2 × 7 improves recovery after spinal cord injury. *Proc. Natl. Acad. Sci. U. S. A.* 106, 12489–12493.
- (69) Itoh, T., Watanabe, N., Ishida, M., Tsuda, Y., Koyano, S., Tsunoi, T., Shimada, H., and Yamada, H. (1998) Stereoselective Disposition of Sulbenicillin in Humans. *Antimicrob. Agents Chemother.* 42, 325–331.
- (70) Hansen, I., Jacobsen, E., and Weis, J. (1975) Pharmacokinetics of sulbenicillin, a new broad-spectrum semisynthetic penicillin. *Clin. Pharmacol. Ther.* 17, 339–347.
- (71) Ward, A., and Richards, D. M. (1985) Cefotetan. *Drugs* 30, 382–426.
- (72) Mazzei, T., Tonelli, F., Anastasi, A., Ficari, F., Novelli, A., and Periti, P. (2004) Tissue Distribution of Cefotetan in Patients with Crohn's Disease. *Chemotherapy* 37, 297–302.
- (73) Garrett, W. S., Gallini, C. A., Yatsunenkov, T., Michaud, M., DuBois, A., Delaney, M. L., Punit, S., Karlsson, M., Bry, L., Glickman, J. N., Gordon, J. I., Onderdonk, A. B., and Glimcher, L. H. (2010) Enterobacteriaceae Act in Concert with the Gut Microbiota to Induce Spontaneous and Maternally Transmitted Colitis. *Cell Host Microbe* 8, 292–300.
- (74) Keighley, M. R. B., Eastwood, D., Ambrose, N. S., Allan, R. N., and Burdon, D. W. (1982) Incidence and Microbiology of Abdominal and Pelvic Abscess in Crohn's Disease. *Gastroenterology* 83, 1271–1275.
- (75) Gautier, R., Douguet, D., Antonny, B., and Drin, G. (2008) HELIQUEST: a web server to screen sequences with specific α -helical properties. *Bioinformatics* 24, 2101–2102.
- (76) Estrela, A. B., and Abraham, W.-R. (2011) Adenosine in the Inflamed Gut: A Janus Faced Compound. *Curr. Med. Chem.* 18, 2791–2815.
- (77) Woody, R. W. (2010) Circular dichroism of intrinsically disordered proteins, in *Instrumental analysis of intrinsically disordered proteins: assessing structure and conformation* (Uversky, V. N., and Longhi, S., Eds.) pp 303–321, John Wiley & Sons, Hoboken, NJ.
- (78) Johansson, J., Gudmundsson, G. H., Rottenberg, M. E., Berndt, K. D., and Agerberth, B. (1998) Conformation-dependent Antibacterial Activity of the Naturally Occurring Human Peptide LL-37. *J. Biol. Chem.* 273, 3718–3724.
- (79) Xhindoli, D., Morgera, F., Zinth, U., Rizzo, R., Pacor, S., and Tossi, A. (2015) New aspects of the structure and mode of action of the human cathelicidin LL-37 revealed by the intrinsic probe p-cyanophenylalanine. *Biochem. J.* 465, 443–457.
- (80) Zsila, F., Bősze, S., Horváti, K., Szigyártó, I. C., and Beke-Somfai, T. (2017) Drug and dye binding induced folding of the intrinsically disordered antimicrobial peptide CM15. *RSC Adv.* 7, 41091–41097.
- (81) Barth, A. (2007) Infrared spectroscopy of proteins. *Biochim. Biophys. Acta, Bioenerg.* 1767, 1073–1101.
- (82) Ismail, A. A., Mantsch, H. H., and Wong, P. T. T. (1992) Aggregation of chymotrypsinogen: portrait by infrared spectroscopy. *Biochim. Biophys. Acta, Protein Struct. Mol. Enzymol.* 1121, 183–188.
- (83) Boye, J. I., Ismail, A. A., and Alli, I. (1996) Effects of physicochemical factors on the secondary structure of β -lactoglobulin. *J. Dairy Res.* 63, 97–109.
- (84) Ishida, K. P., and Griffiths, P. R. (1993) Comparison of the Amide I/II Intensity Ratio of Solution and Solid-State Proteins Sampled by Transmission, Attenuated Total Reflectance, and Diffuse Reflectance Spectrometry. *Appl. Spectrosc.* 47, 584–589.
- (85) Ricci, M., Horváti, K., Juhász, T., Szigyártó, I., Török, G., Sebák, F., Bodor, A., Homolya, L., Henczkó, J., Pályi, B., Mlinkó, T., Mihály, J., Nizami, B., Yang, Z., Lin, F., Lu, X., Románszki, L., Bóta, A., Varga, Z., Bősze, S., Zsila, F., and Beke-Somfai, T. (2020) Anionic food color tartrazine enhances antibacterial efficacy of histatin-derived peptide DHVAR4 by fine-tuning its membrane activity. *Q. Rev. Biophys.* 53, e5.
- (86) Georgiou, C. D., Grintzalis, K., Zervoudakis, G., and Papapostolou, I. (2008) Mechanism of Coomassie brilliant blue G-250 binding to proteins: a hydrophobic assay for nanogram quantities of proteins. *Anal. Bioanal. Chem.* 391, 391–403.
- (87) Kohut, G., Sieradzan, A., Zsila, F., Juhász, T., Bősze, S., Liwo, A., Samsonov, S. A., and Beke-Somfai, T. (2019) The molecular mechanism of structural changes in the antimicrobial peptide CM15 upon complex formation with drug molecule suramin: a computational analysis. *Phys. Chem. Chem. Phys.* 21, 10644–10659.
- (88) Kiss, É., Gyulai, G., Pári, E., Horváti, K., and Bősze, S. (2018) Membrane affinity and fluorescent labelling: comparative study of monolayer interaction, cellular uptake and cytotoxicity profile of carboxyfluorescein-conjugated cationic peptides. *Amino Acids* 50, 1557–1571.
- (89) Ziegler-Heitbroc, H. L., Thiel, E., Futterer, A., Herzog, V., Wirtz, A., and Riethmüller, G. (1988) Establishment of a human cell line (Mono Mac 6) with characteristics of mature monocytes. *Int. J. Cancer* 41, 456–461.
- (90) Chen, T., Drabkowski, D., Hay, R., Macy, M., and Peterson, W., Jr (1987) WiDr is a derivative of another colon adenocarcinoma cell line, HT-29. *Cancer Genet. Cytogenet.* 27, 125–134.
- (91) Liu, Y., Peterson, D. A., Kimura, H., and Schubert, D. (1997) Mechanism of cellular 3-(4, 5-dimethylthiazol-2-yl)-2, 5-diphenyltetrazolium bromide (MTT) reduction. *J. Neurochem.* 69, 581–593.
- (92) Mosmann, T. (1983) Rapid colorimetric assay for cellular growth and survival: application to proliferation and cytotoxicity assays. *J. Immunol. Methods* 65, 55–63.
- (93) Slater, E. C. (1963) Relation between Energy Supply and Energy Demand in the Living Cell. *Ned. Tijdschr. Geneesk.* 107, 1543–1544.
- (94) Micsónai, A., Wien, F., Kernya, L., Lee, Y.-H., Goto, Y., Réfrégiers, M., and Kardos, J. (2015) Accurate secondary structure prediction and fold recognition for circular dichroism spectroscopy. *Proc. Natl. Acad. Sci. U. S. A.* 112, E3095–E3103.